V. Campbell

Technical Information Report #154

A MODEL FOR A LIGHT VALVE PROJECTOR

by:

R. G. Hiller

TVRD

5/5/61

Supersedes T. I. R. #145 and T. I. R. #148

A simplified model of a light valve projector was devised and then analyzed by means of Fourier transformation techniques. Since the basic components of the device are a phase grating formed on a thin film of transparent oil and a schlieren optical system, the analysis was divided into two major topics. These being: 1) the optical conversion efficiency of a sinusoidal phase grating and 2) the effects of schlieren optics on optical transient response. The former topic included both dynamic and instantaneous characteristics. The efficiencies predicted correlated remarkably well with experiment when the two were compared. As a result the sinusoidal grating has been used as a model for the oil surface in the development of the projector.

When Fourier transformation was applied to the model in an effort to determine the transient response of the projector, it was seen that the analysis of the model was very similar to the analysis of low pass filters in network theory. This analogy was subsequently used to predict the resolution of the projector. When these predictions were compared to observations made on the projector, discrepancies on the order of 30-50% resulted. The filter theory was modified in an effort to improve the situation. This was to no avail, however. It was theorized that a modification in the assumption concerning the light source used in the model would result in more reliable predictions of operation. Time did not permit a complete investigation of the problem. Hence, the modification was left in the form of a recommendation to any one who might want to continue in the analysis.

CONTENTS

Preface i

I. The Projector 1

II. The Model to be Analyzed 3

III. Optical Conversion Efficiency of the Grating 5

IV. Spatial Transient Response of the System 15

V. Conclusion 27

Appendices

A. Schlieren Optics 32

B. An Electrical Analogy for the Projector 34

Illustrations 36

Bibliography 49

PREFACE

The object of this work was not to perform an analysis of the projector that would include second and third order effects. It was undertaken in an effort to devise the simplest model that would explain the phenonema already observed and that could be used to predict the results of modifications that were to be made in the process of developing the device.

It is hoped that this has been accomplished. If it has not, it is my sincere hope that the work done can be used as a basis for further analysis that may be undertaken.

None of the work would have been possible with out the guidance and cooperation of my thesis advisor, Dr. S. T. Jutila, and the many men of General Electric with whom I consulted during the course of this analysis. The two men who shared the brunt of this should be singled out for individual recognition. Dr. W. E. Good and Mr. T. T. True.

I. THE PROJECTOR

The basic components of this projector are a thin film of transparent oil and a schlieren optical system. The oil film is spread on a glass disc which has had a conductive coating applied to it. By scanning the raster or oil surface with an electron beam, a charge is deposited in the oil. This charge is attracted to the conductive coating and the oil surface is deformed. Two types of scanning processes are used to deposit the charge. The simpler of the two is to scan the raster in much the same way as a normal television picture tube. This produces lines of charge oriented along the scan lines. The second method is to velocity modulate the beam as it scans along a line. This velocity modulation will produce a varying charge distribution along the line. This produces lines of charge that are perpendicular to the scan lines. It is much easier to produce varying grating frequencies and amplitudes with the latter method. The frequency is controlled by the modulating frequency and the amplitude by the amplitude of the modulating signal. The measurements taken for the work in Appendix A were for a grating of the latter type. Since the charge deposited on the oil slowly leaks off to the conductive coating, the modulation decays at some finite rate.

The schlieren system used is a multiple slit system. (See Appendix A for a further explanation of the schlieren system)

Typical input slit dimensions are: .025" wide slits on .045" Centers. Some typical output slit dimensions are: .016" slits on .044" centers.

II. THE MODEL TO BE ANALYZED

Instead of analyzing the projector itself, a simplified model will be investigated. First to be considered will be the oil film or raster. The film will be assumed to have a sinusoidal cross-section with a spatial frequency of 1/d. Only two dimensions will be considered, the thickness of the oil film (y) and the displacement from the axis of the system (x). The grating will be assumed to be symmetrical about this axis, (x = 0). The oil will be assumed to be perfectly transparent. The formation of the grating is not important except that it is formed in a negligible time and then decays at some finite rate. The process repeats every T sec. This period, for all practical purposes, can be considered equal to the normal television field time, (1/60 sec). Both exponential and linear decay modes will be investigated. The ratio of the depth of modulation on the oil (A) to modulation period (d), is about 1:100, both in the actual projector and the model. Figure #1 is a sketch of such an oil surface.

The schlieren system was simplified considerably in devising the model. In the model, only a single input slit is used. This is assumed to be narrow enough to permit the assumption of light emitted from it to be coherent. The schlieren lens is split into two parts, (each of which is assumed to be a perfect lens), with the raster being placed between them. The input slit is

placed in the focal plane of one, and is centered on the system axis. The output bars are then placed in the focal plane of the second, again centered about the system axis. This is done so that the raster is illuminated with normally incident light. The incident light will be assumed monochromatic, as well as coherent. By assuming unity magnification of the projection system for the raster and its image, no scale factor need be introduced between them. (i.e., $x = x''$). The output bars to be considered range from a set utilizing only the first order diffraction to a set utilizing all orders except the zero or central order. These will be described as they are considered. Figure #2 is a sketch of the model.

III. OPTICAL CONVERSION EFFICIENCY OF THE GRATING

Since the oil surface has been assumed to be perfectly transparent, the conversion efficiency of the grating is the ratio of the intensity of the light utilized to the intensity of the light incident on the output bars (i.e., output/input).

The conversion efficiency will be determined by applying Fourier transformation techniques.[1,2] The length of the grating to be considered is very large in comparison to the period of one of the sinusoids. Since the grating in the model is illuminated with a normally incident plane wave of monochromatic, coherent, light the light distribution in the focal plane of the schlieren lens (output bars) is given by[3,4]:

$$\text{Eq. 1} \quad F(x') = \int_{-L/2}^{L/2} f(x)\, e^{j\frac{2\pi x x'}{\lambda F}}\, dx$$

where L = length of grating

λ = wavelength of incident light

F = focal length of the schlieren lens

f(x) = function describing the effect of the grating on incident light.

The function f(x) will be determined by using the method employed

---

[1] E. L. O'Neill, The Analysis and Synthesis of Linear Coherent and Incoherent Optical Systems. Boston University, 7/55.

[2] E. L. O'Neill, Selected Topics in Optics and Communications Theory. Boston, Physical Research Lab. ITEK Corp., 9/58.

[3] J. R. Horsch, Lens Utilization in Coherent Optical Data Processing. Syracuse, TIS #R60 ELS-21, 3/15/60.

[4] R. V. Pole, An Optical Analysis of Surface Deformation Recordings.

in work done by R. A. Powell and H. Poritsky of General Electric, General Engineering Laboratory, Schenectady, New York. The function f(x) will be determined by considering the disturbance produced by the grating on a normally incident plane wave passing through the grating incident on a plane at $y = S > h + A$. ($h + A$ = maximum possible thickness of oil, see diagram of oil surface). The phase angle of the light at $y = 0$ will be assumed to be zero. The light incident on $y = S$ can now be expressed by Eq. 2.

Eq. 2 $\quad C \epsilon^{j\phi_s}$

where C = amplitude of light wave

ϕ_s = phase shift encountered in travelling from y = 0 to y = S

ϕ_s in turn may be given by the sum:

Eq. 3 $\quad \phi_s = \phi_1 + \phi_2$

where ϕ_1 = phase shift in oil

ϕ_2 = phase shift outside of oil

ϕ_1 and ϕ_2 are given by Equations 4 and 5.

Eq. 4 $\quad \phi_1 = \frac{2\pi}{\lambda_1}\left[h + A \sin\left(\frac{2\pi}{d}\right)x\right]$

Eq. 5 $\quad \phi_2 = \frac{2\pi}{\lambda_2}\left[S - h - A \sin\left(\frac{2\pi}{d}\right)x\right]$

where λ_1 = wavelength in oil

λ_2 = wavelength outside of oil

Since the index of refraction outside of the oil is unity, the following expressions hold.

Eq. 6 $$\lambda_1 = \lambda = \frac{\lambda_2}{n}$$

Eq. 7 $$\phi_s = \frac{2\pi}{\lambda}\left[S + (n-1)(h + A\sin 2\pi x/d)\right]$$

The term S + (n-1)h represents a constant phase shift with respect to x and, therefore, may be incorporated into the constant C. Consequently, the expression for the light incident on y S is actually f(x) as shown in Eq. 8.

Eq. 8 $$f(x) = C\epsilon^{j\frac{2\pi}{\lambda}(n-1)A\sin\left(\frac{2\pi}{d}\right)x}$$

Recognizing that[5]

Eq. 9 $$\epsilon^{jz\sin x} = \sum_{-\infty}^{\infty} J_k(z)\,\epsilon^{jkx}$$

where $J_k(z)$ is the kth order Bessel function of the first kind with argument z.[6,7]

f(x) can be expressed as:

$$f(x) = \sum_{-\infty}^{\infty} J_k(z)\,\epsilon^{j\frac{k2\pi x}{d}}$$

---

[5] S. Goldman, Transformation Calculus and Electrical Transients. N. Y., Prentice-Hall, 1949.

[6] F. B. Hildebrand, Advanced Calculus for Engineers. New York, Prentice-Hall, 1948.

[7] Jahnke and Emde, Tables of Functions. New York, Dover Publications, 1943.

where $z = 2\pi/\lambda\,(n-1)$

If this is substituted into the expression for F(x'), Eq. 3, and the integral evaluated, F(x') becomes:

$$\text{Eq. 10}\quad F(\psi) = C\left[\sum_{-\infty}^{\infty} \frac{J_k(z)\, e^{j2\pi\left(\frac{\psi'}{\lambda F}+\frac{k}{a}\right)\psi}}{j2\pi\left(\frac{\psi'}{\lambda F}+\frac{k}{a}\right)}\right]\Bigg|_{-1/2}^{1/2}$$

$$= C\lambda \sum_{-\infty}^{\infty} J_k(z)\,\operatorname{sinc}\,\pi\lambda\left(\frac{\psi'}{\lambda F}+\frac{k}{a}\right)$$

where $\operatorname{sinc} x = \frac{\sin x}{x}$

Eq. 11 expresses the intensity variation of the light displayed on the output schlieren bars.[8]

$$\text{Eq. 11}\quad I(x') = \left|F(x')\right|^2$$

$$= \left|C\lambda\right|^2\left[\sum_{-\infty}^{\infty} J_k(z)\,\operatorname{sinc}\,\pi\lambda\left(\frac{\psi'}{\lambda F}+\frac{k}{a}\right)\right]^2$$

If it is assumed that $J_L >> d$, the term $\operatorname{sinc}\,\pi\lambda\left(\frac{\psi'}{\lambda F}+\frac{k}{a}\right)$ has negligible value for $x' \neq k\lambda F/d$ and has a value of unity for $x' = k\lambda F/d$. Consequently, the display becomes that ordinarily associated with diffraction gratings. This being a set of discrete

---

[8] Max Born and Emil Wolf, Principles of Optics. New York, Pergamon Press, 1959

lines at intervals of λ F/d along the output bars. The line at $x = k \lambda F/d$ is the kth order of diffraction and its intensity is given by $J_k^2(z)$. By noting that for $z = 0$, $I(0) = |CL|^2$, it can be seen that $|CL|^2$ represents the intensity of all the light incident on the output bars or the input in our efficiency equation. It can be seen that the efficiency of the kth order of diffraction is now given by Eq. 12.

$$\text{Eq. 12} \quad \text{Eff} = J_k^2(z)$$

From Eq. 13 it can be seen that the spectral display is symmetrical about $x' = 0$.[7]

$$\text{Eq. 13} \quad (-1)^k J_k(z) = J_{-k}(z)$$

where n is an integer 1, 2, 3.....

Consequently, the efficiency of the kth order is redefined by Eq. 14.

$$\text{Eq. 14} \quad \text{Eff} = 2 J_k^2(z) \text{ for all orders except zero}$$

$$= J_0^2(z) \text{ for zero order}$$

Of course, k will now be restricted to positive values since this definition of efficiency includes the spectral lines at $x' = k \lambda F/d$ and $x' = -k \lambda F/d$. The conversion efficiencies for each diffraction

---

[7] Jahnke and Emde, Tables of Functions. New York, Dover Publications, 1943.

order as a function of $z \propto \pi/\lambda\,(n-1)$ has been plotted in Figure 3. In Figure 4, the conversion efficiency for four output bar arrangements is plotted as a function of z. These four arrangements are: 1) a set utilizing only the first order diffraction, 2) a set utilizing the first and second orders, 3) a set utilizing the first, second and third orders and, 4) a set utilizing all orders except the zero or central order. The last set of bars would have the highest efficiency theoretically possible since they utilize all the light that can be used and still retain the operating characteristics of the device. As stated earlier, the scanning process involved in this projector produces dynamic effects that must be accounted for. Since the rise time associated with the formation of the oil surface has been assumed negligible compared to the decay time and the grating, in a steady state situation, is rewritten every T sec. (the time taken to completely scan the raster area once), the average efficiency is given by Eq. 15.

$$\text{Eq. 15} \quad \overline{\text{Eff}} = \frac{2}{T} \int_0^T \sum_n J_k^2 [z(t)] \, dt$$

where the summation is made for the orders utilized by the schlieren output bars and $z(t)$ represents the dynamic characteristics of z. Two modes of decay are to be considered: 1) a linear decay to zero during T, $z(t) = z_0(1-t/T)$, and, 2) an exponential decay with time constant

τ, $z(t) = z_0 \epsilon^{-t/\tau}$. Three representative exponential decays will be considered.

1) decay from z_0 to z_0/ϵ $\frac{1}{2}$(τ = 2 T a viscous oil)

2) decay from z_0 to z_0/ϵ (τ = T)

3) decay from z_0 to z_0/ϵ^2 ($\tau = \frac{T}{2}$ a non-voscous oil)

The factor z_0 represents the initial amplitude of modulation as indicated by Eq. 16.

$$\text{Eq. 16} \quad z_0 = \frac{A_0}{\lambda} (2\pi)(n-1)$$

where A_0 = initial amplitude.

A few comments concerning the conversion efficiency curves will be made before continuing. The peak instantaneous efficiency of the system may be increased considerably from 67% to 93% by utilizing the first and second orders instead of the first only. If the third order is also included, the peak instantaneous efficiency is increased by another 6%, to 99%. The two systems using higher orders do not deviate from the theoretical maximum efficiency until the peak efficiency of each curve is approached. The first order curve starts to fall away at about half its peak value (38%), however. It would seem that the average curves should be predictable from an examination of the instantaneous curves. For a viscous oil the

amplitude will not decay very much from the initial value, (z_0). Consequently, the intensity will remain fairly constant over the interval (T) resulting in an average efficiency curve that follows the instantaneous curve rather closely. The instantaneous curves correspond to an infinite time constant, in other words. For the other extreme, a non-viscous oil, the modulation will decay to a very small value during each interval (T). This results in the average being taken over a wide range of efficiency or z. Consequently, any rapid fluctuations in the instataneous curves will be smoother out and the peak average efficiency will be somewhat lower than that for the viscous oil. For any exponential decay, the efficiencies corresponding to values of z toward the end of the interval are weighted more than those at the beginning of the averaging interval. This should produce a delay of the average efficiency curves behind the instantaneous efficiency curves when plotted as a function of z. The decay should become more pronounced as the magnitude of the decay increases (oil viscosity decreases). For a linear and exponential decay between the same points, this phenomenon should produce a similar delay of the average curve for an exponential decay behind the average for a linear decay.

Figures 5-8 are plots of the average efficiencies for the

decays and bar systems described earlier. It can be seen that the average curves follow the predictions made previously. The analog computer at General Electric, HMED, Syracuse, was used to evaluate the integral:

Eq. 17 $$\int_0^t J_k^2(z)(t)\,dt$$

The average curves were then determined by calculating points for Figures 5-8 from this integral. The curves for the time constant equal to one field length were also calculated on an IBM 610 digital computer at General Electric, TVRD, Syracuse.

As stated previously, only a small increase in peak efficiency is realized by using the first three orders instead of the first two. For the average efficiency using an oil having a time constant equal to T, the peak efficiency is increased from 59% to 84% by using the first and second orders instead of the first only. A furhter increase of peak efficiency to 91% is realized by including the third order as well.

The curve shown in Figure 12 is an attempt to simulate the gamma correction normally applied to video signals. The assumption that the modulation amplitude (A) is proportional to the applied video signal was made in determining these curves. Upon examination of any of the average efficiency curves, it is seen that on small

levels of modulation, the efficiency curve approaches a kz^2 curve. For higher levels, however, it seems to approach a $kz^{\frac{1}{2}}$ curve. Consequently, for the normal gamma correction factor of 2.2, the efficiency curve should be more linear at low levels and the non-linearity exaggerated at high levels of z. This is seen to be the case. For efficiencies much greater than 50%, the non-linearity becomes so extreme as to be proven disasterous by producing a "wash-out" of highlights. The ideal situation would be an applied signal with normal correction at low levels but with an inverse of the normal gamma correction at higher levels. Since this is highly impractical, the system should be operated with a peak efficiency of about 50% to insure a proper contrast ratio at highlights.

IV. SPATIAL TRANSIENT RESPONSE OF THE SYSTEM

Fourier transformation techniques will again be used in this portion of the analysis. Before, the only display investigated was that in the focal plane of the schlieren lens (output bar plane). The image of the raster becomes important now, however. This image will be represented by the function f(x") which is a function describing the light distribution on the projection screen (raster image plane). Since unity magnification was assumed between the raster and its image, f(x") is given by the Fourier transformation of Eq. 18.[1,2]

$$\text{Eq. 18} \quad f(x'') = \frac{1}{2\pi} \int_{-\infty}^{\infty} F(\omega)\, G(\omega)\, \epsilon^{j\omega x''}\, d\omega$$

where $\omega = 2\pi x'/\lambda F$

λ and F as before (Eq. 1)

$G(\omega)$ is a function describing the output bar geometry as a function of ω (x').

$F(\omega)$ is of course Eq. 1 with ω replacing $2\pi x'/\lambda F$ or:

$$\text{Eq. 19} \quad F(\omega) = \int_{-1/2}^{1/2} f(x)\, \epsilon^{j\omega x}\, dx$$

Now ω_0 will be defined as $2\pi/d$ so that f(x) becomes:

---

[1] E. L. O'Neill, The Analysis and Synthesis of Linear Coherent and Incoherent Optical Systems. Boston University, 7/55.

[2] E. L. O'Neill, Selected Topics in Optics and Communications Theory. Boston, Physical Research Lab. ITEK Corp., 9/58.

Eq. 20 $f(x) = \epsilon^{j z \sin \omega_0 t} = \sum_{-\infty}^{\infty} J_k(z) \epsilon^{j k \omega_0 t}$

with $z = A(2\pi/\lambda)(n-1)$ as before

The length of the grating (L) will be expressed in terms of the period of the sinusoidal cross-section (Figure 1) as:

Eq. 21 $L = 2md$

Now if equations 19-21 are combined in the proper manner, $F(\omega)$ can be evaluated to be:

Eq. 22 $F(\omega) = 2 \sum_{-\infty}^{\infty} J_k(z) \frac{\sin md(\omega + k\omega_0)}{(\omega + k\omega_0)}$

An investigation of Eq. 22 reveals that this is a series of $\frac{\sin nx}{x}$ functions centered at intervals of ω_0 or $\lambda F/d$ along the output bar plane. (This plane has become a frequency domain with x and x" planes becoming time domains in the usual sense). Each of these $\frac{\sin nx}{x}$ distributions has a peak amplitude of $2 J_k(z)$ at $\omega = -k\omega_0 (x = -k \lambda F/d)$. If md is large enough each of the distributions can be thought of as a discrete distribution of light centered at $\omega = -k\omega_0$. Or, in other words, for such a situation the light represented by $2 J_k(z) \frac{\sin md(\omega + k\omega_0)}{\omega + k\omega_0}$ can be associated with the kth order of diffraction if md is large enough. For small values of md the $\frac{\sin nx}{x}$ distributions begin to overlap

considerably so that discrete diffraction orders cannot be distinguished and the light distribution on the output bars becomes continuous. Using Rayleigh's criterions[9], this will occur for $m < 1$. If this restriction is met ($m < 1$), it is seen that a set of output bars that had slits centered at $\omega = Ik\,\omega_0$ would be necessary and sufficient to tuilize the kth order diffraction. A set of bars that would utilize only the first order diffraction is shown below.

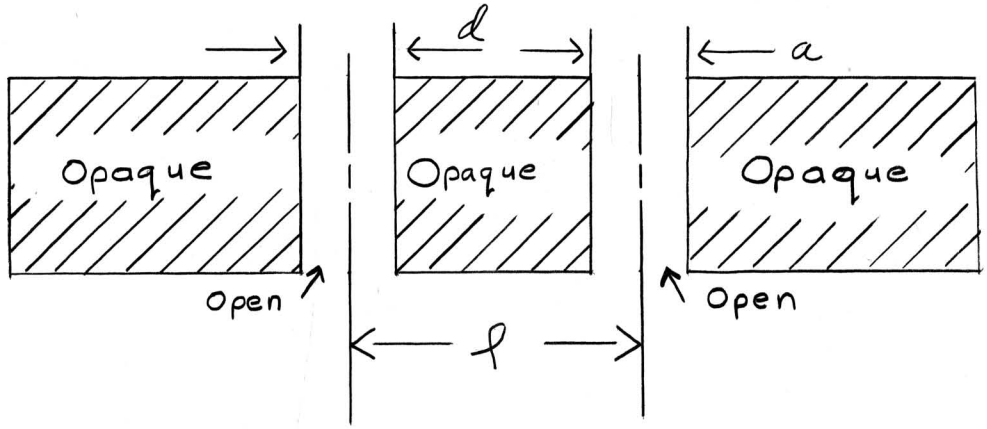

$$\ell = 2\lambda F/d = \omega_0 \lambda F/2\pi$$

$$\beta = a/\ell$$

These set of output bars will be used in the following analysis

It can be shown that for $m > \frac{1}{2}$ and $\beta < 1/3$, any light passing through the slits from diffraction orders other than the first is negligible. Consequently, only the first order light

---

[9]Jenkins & White, Fundamentals of Optics. New York, McGraw-Hill,

will be considered in performing the inverse transformation of Eq. 18. $G(\omega)$ can easily shown to be:

$$\text{Eq. 22} \quad \left.\begin{aligned} G(\omega) &= 1 \\ &= 0 \end{aligned}\right\} \quad \begin{aligned} &\text{for } \omega_0 \frac{-\pi a}{\lambda F} < |\omega| < \omega_0 + \frac{\pi a}{\lambda F} \\ &\text{for all other } \omega \end{aligned}$$

Now with the statement made above in mind, $f(x'')$ becomes:

$$\text{Eq. 23} \quad f(x'') = \frac{1}{2\pi} \int_{-\omega_0 - \frac{\pi a}{\lambda F}}^{-\omega_0 + \frac{\pi a}{\lambda F}} 2 J_1(z) \frac{\sin \pi d(\omega + \omega_0)}{\omega + \omega_0} \epsilon^{j\omega x''} d\omega$$

$$+ \frac{1}{2\pi} \int_{\omega_0 - \frac{\pi a}{\lambda F}}^{\omega_0 + \frac{\pi a}{\lambda F}} J_{-1}(z) \frac{\sin \pi d(\omega - \omega_0)}{(\omega - \omega_0)} \epsilon^{j\omega x''} d\omega$$

Upon a change in variable $f(x'')$ is seen to be:

$$\text{Eq. 24} \quad f(x'') = \frac{1}{\pi} \int_{-\frac{\pi a}{\lambda F}}^{\frac{\pi a}{\lambda F}} J_1(z) \frac{\sin}{y} y \pi d \epsilon^{j(y - \omega_0)x''} dy$$

$$+ \frac{1}{\pi} \int_{-\frac{\pi a}{\lambda F}}^{\frac{\pi a}{\lambda F}} J_{-1}(z) \frac{\sin}{y} y \pi d \epsilon^{j(y - \omega_0)x''} dy$$

Then since $J_1(z) = -J_{-1}(z)$

$$\text{Eq. 25} \quad f(x'') = -2j \frac{J_1(z) \sin \omega_0 x''}{\pi} \int_{-\frac{\pi a}{\lambda F}}^{\frac{\pi a}{\lambda a}} \frac{\sin}{y} \; y\, m d\, \epsilon^{jyx} d y$$

$$= -2j\, J_1(z) \sin \omega_0 x'' \left[Si \frac{\pi a}{\lambda F} (x'' + md) - \frac{Si\, \pi a}{\lambda F} (x'' - md) \right]$$

where $Si(x) = \int_0^x \frac{\sin z}{z} \, dz$

This expression can be broken up into two components

25 a) a carrier $-2j\, J_1(z) \sin \omega_0 x''$

25 b) and an envelope

$$\frac{1}{\pi} \left[Si \frac{\pi a}{\lambda F} (x'' + md) - Si \frac{\pi a}{\lambda F} (x'' - md) \right]$$

The envelope is seen to be nothing more than the response of a zero phase shift perfect low filter to a pulse input.[10] The perfect low filter, of course, has no attenuation in its pass band and has an infinite slope at the cutoff frequency. The bandwidth for this case would be $\pi a / \lambda F$ and the input pulse has a duration of

---

[10] S. Goldman, Frequency Analysis, Modulation and Noise. New York, McGraw-Hill Book Co., 1948.

2 md which is merely the length of the grating being considered. Since the envelope of the projector response will be sufficient to describe the transient response, this analogy with filter theory will be used to determine the transient response. This will be accomplished by first determining the bandwidth of the output bars ($\pi a/\lambda$ F) and then determining what the response of a low pass filter with this bandwidth to a pulse of duration 2 md would be. This response is then the envelope of f(x") as described above.

This represents the complex wave representation of the raster image. Since the eye is not sensitive to phase variation of light, but to intensity variation only, f(x") is not the image seen by the eye. This problem is easily solved though when it is recognized that the intensity variation I(x") is:

$$\text{Eq. 26} \quad I(x'') = \left| f(x'') \right|^2$$

The intensity envelope is seen to be merely the square of 25 b.

One of the applications of this projector is a television receiver. Consequently the response to the three usual television test signal were determined. These are, 1) a step function (response to a discontinuity), 2) a single pulse (response to isolated detail), and 3) a double pulse (response to repeated

detail or resolution). It was assumed that the electronics involved in forming the grating was sufficient to produce the grating modulation envelopes shown below.

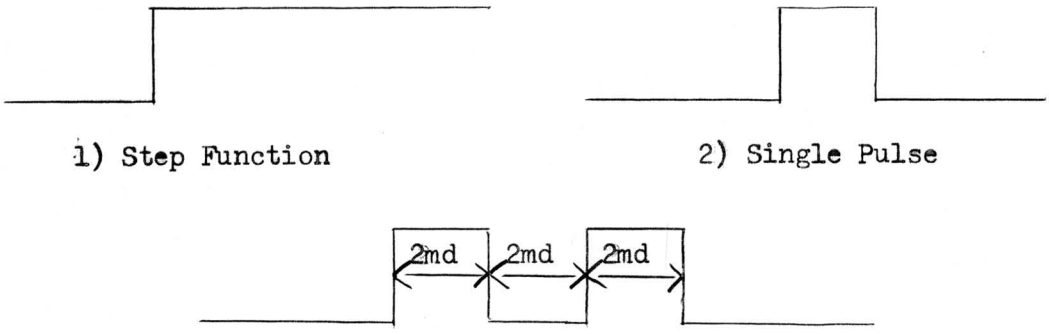

1) Step Function

2) Single Pulse

3) Double Pulse

The responses calculated by using the filter theory analogy outlines previously for these three situations are shown in Figures 9-11. For each input signal various output bar slit widths were considered. Since the center to center spacing of the slits (ℓ) remains constant these different slits widths are represented by the parameter $\beta = a/\ell$ (a = slit width). In each case the input signal is shown so that the response can be compared to it more easily. For the single and double pulse inputs the relationship between the bandwidth of the slit (β) and the grating length (m) is given.

This makes the curves applicable to any system where λ, d and F are known since:

Eq. 27 $\rho = 2\lambda F/d$

$\beta = 1/3$ was the largest value investigated since for any larger value the assumptions concerning the "spill-over" of orders other than the first into the output slit began to fall down.

By representing repeated detail as a square wave with a frequency $\frac{1}{4md}$ (see sketch below) the resolution (ability to resolve repeated detail) can be determined from the filter analogy.

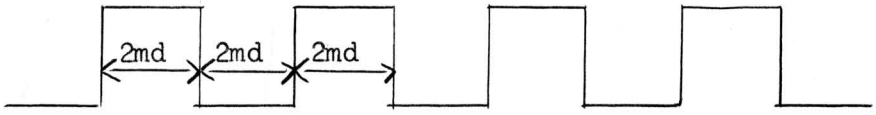

Grating envelope for resolution investigation

It will be assumed that if the bandwidth of the output slit is sufficient to pass the fundamental harmonic of the Fourier series for this square wave, the detail will be resolved. The limit of resolution is, therefore, given by:

Eq. 28 $a/\lambda F = \frac{1}{2} md$

Substituting Eq. 27 into this yields:

Eq. 29 $\beta = \frac{1}{4} m$

Since each of the lines which is resolved consists of 2 m grating lines, the resolution in lines/in is given by:

Eq. 30 $\frac{1}{2} md$

Substituting Eq. 29 results:

Eq. 31 $R = 2\beta/d$ lines/in

where 1/d grating spatial frequency

It will be remembered that the foregoing analysis was performed for the situation where the diffraction order was centered in the output slit. If the diffraction order is not centered at $x' = I\rho/2$ but $x' = I\rho/2 + \frac{\gamma a}{2}$ instead, the low pass filter theory can still be used to analyze the situation. Now, however, the low pass filter is unsymmetrical and Eq. 32 represents the response, f(x"), of the device.

Eq. 32 $f(x'') = j \frac{J_1(z)}{\pi} \sqrt{\rho^2 + Q^2} \sin(\omega_0 x'' + \phi)$

where $$P = \left[Si\,\frac{\pi a}{\lambda F}(1-\gamma)(x''+md) + Si\,\frac{\pi a}{\lambda F}(1+\gamma)(x''+md) - Si\,\frac{\pi a}{\lambda F}(1-\gamma)(x''-md) - Si\,\frac{\pi a}{\lambda F}(1+\gamma)(x''-md) \right]$$

$$Si(x) = \int_0^x \frac{\sin z}{z}\,dz$$

$$Q = \left[Ci\,\frac{\pi a}{\lambda F}(1-\gamma)(x''+md) - Ci\,\frac{\pi a}{\lambda F}(1+\gamma)(x''+md) + Ci\,\frac{\pi a}{\lambda F}(1+\gamma)(x''-md) - Ci\,\frac{\pi a}{\lambda F}(1-\gamma)(x''-md) \right]$$

$$Ci(x) = -\int_x^\infty \frac{\cos z}{z}\,dz$$

$$\phi = \tan^{-1} Q/P$$

The term $\frac{1}{\pi^2} P^2 + Q^2$ represents the intensity envelope. This assymmetry should produce an increase in resolution, and a degradation of transient response if the analogy with filter theory is valid.[10]

---

[10] S. Goldman, Frequency Analysis, Modulation and Noise. New York, McGraw-Hill Book Co., 1948.

The procedures described here could be extended to include additional diffraction orders other than the first. This would probably involve the use of a multiple slit output bar arrangement. The bandwidth to be associated with the slits for each order would have to be determined and an $f(x'')$ then determined for each order. These would then be summed and the envelope of this sum determined. Squaring this would then give the desired response envelope.

Care would have to be exercised to insure that all the assumptions made in this analysis were still valid. If they were not, the procedure would have to be modified accordingly.

If higher orders were to be considered the carrier shown in 25a would be changed considerably. For the kth diffraction order it would be of the form:

Eq. 33 $2 J_k(z) \sin k \omega_0 x''$ (k odd), or

$2 J_k(z) \cos k \omega_0 x''$ (k even)

When $I(x'')$ is found from $\left|f(x'')\right|^2$, the carrier for $I(x'')$ becomes:

Eq. 34 $2 J_k^2(z) \left[1 + (-1)^k \cos 2 k \omega_0 x''\right.$

For the first order situation analyzed it is seen that the image of the raster would appear at twice the original grating frequency.

Each additional order used would contribute another sinusoid at 2^k the original grating frequency, where the kth order is used.

V. CONCLUSIONS

The best method of judging the worth of a model such as this is by how well the model predicts experimental observations. This model achieved this by varying degrees of success. The predicted conversion efficiencies (both static and dynamic) correlated remarkably well with experimental data. The transient response and resolution predictions left something to be desired, however. This has been attributed to an oversimplification of the projector in devising the model.

All measurements were taken on a projector which formed the grating by velocity modulating the electron beam. The modulation signal was an r.f. voltage in the 7-8 Mcs. range. This has been used as the independent variable in plotting the experimental data. Figure 13 is a plot of efficiency measurements taken by W. E. Good and T. T. True. The theoretical curves shown here were plotted by matching zeroes and maxima and assuming (z), and therefore grating depth, to be proportional to the r. f. signal applied to the deflection plates. It can be seen that for $z < 3.5$, the experimental results follow theory quite well. Beyond this point, the grating probably either becomes non-sinusoidal or linearity between (z) and r. f. voltage ceases. Efficiency measurements taken as a function

of time rather than r. f. signal follow the Bessel function prediction for higher values of z, however. Consequently, the latter situation probably explains the grating formation more closely. Figure 14 shows a plot of (z) vs. time as the modulation decays. These measurements were taken from the work mentioned previously. This plot substantiates the assumption of exponential decay over the useful range of (z). The line drawn in this figure has a time constant of approximately one field length (1/60 sec). The grating used for these measurements was formed with a modulation frequency of 7.0 Mc/s. With a raster width of 1.5" the grating spacing was 4.35 mils. This corresponds to a spatial frequency of 230 lines/in (T. V.). The oil used, G. E. Silicone Products, #398-14-1142, had a viscosity of 330 centistokes.

By matching the peak measured average efficiencies with corresponding calculated values, the plot of (z) vs. r. f. voltage shown in Figure 15 was obtained. Again, the theory of linear grating formation is substantiated. With this curve as a basis, the theoretical and experimental average efficiencies for the first and second diffraction orders were plotted in Figure 16. Except for the peak values, theory and experimental results seem to agree quite well. The measurement of average efficiencies were taken by

J. Bebris and W. Bates on 12/5/60. The grating was formed on G. E. Silicone Products oil, #301-114-1179 with an 8.4 Mc/s. (d = 3.0 mils) modulation signal. This oil had a viscosity of 400-450 centistokes.

The light output of the first order may be used to measure the decay of the oil with a good degree of confidence. It will be noticed in Figure 3 that the efficiency (light output) of the first order is nearly proportional to (z) for $0.5 < z < 1.4$. Consequently, the decay characteristics of the light in first order can be assumed to be the same as those of the oil if measurements are made in this region of linearity. Using this technique, the time constant of the second oil was determined to be equal to that of the first (1/60 sec).

Measurements taken on the present projector indicate that peak efficiency decreases with increasing grating frequency. This is also predicted in work done by S. T. Jutila. He predicts that peak efficiency is constant up to a cutoff frequency. Beyond this cutoff, the peak efficiency decreases rapidly with increasing grating frequency. The cutoff frequency is primarily a function of electron beam spot size. The measurements taken were for grating frequencies in the region of cutoff which might explain the measured efficiencies being somewhat lower than predicted by theory.

Discrepancies on the order of 30-50% occurred when the resolution predicted from theory was compared to observations made on the projector. The predicted resolution was lower than that observed (166 lines predicted, 250 observed and 215 predicted and 325 observed). It was hoped that the unsymmetrical filter analogy proposed, Eq. 32, would explain the discrepancy. The increase in resolution predicted by this was far too great (600 lines predicted, 375 observed). Time did not permit a complete investigation to determine the exact cause of discrepancy. It is felt that a few refinements made on this model would result in a model that would predict the projector response with a good degree of reliability. The major refinement would be a modification of the assumption that the light from the input slot is coherent. In making this assumption it was implied that the input slit represented a line source of light. Instead of a single line source, the input slit could be assumed to consist of a series of line sources placed side by side. These sources would be incoherent with respect to one another. An intensity response would be determined for each of these sources. Then these responses would be summed to give the system response. Some provision might be made for the polychromatic nature of the input light. This would probably be a second order effect, however.

The use of a single input slit instead of multiple slits most likely introduces second order error, as well. Consequently, no investigation was made of this problem. This effect can be determined from work done on the effects of multiple slit operations on imaging systems.[11,12]

---

[11] Effects of Aperture Slits on the Quality of Projected Image, J. M. Holeman, TIS #60GL169, 8/22/60

[12] Diffraction Patterns and Sine Wave Response Functions for Slit Type Apertures, D. DeJager, TIS #60GL123, 6/17/60

APPENDIX A

SCHLIEREN OPTICS

The eye cannot detect phase variations present in light. It is sensitive only to intensity variations. Hence, some means must exist for transforming the phase variations impressed by the grating on the incident light into intensity variations. This is the purpose of the schlieren optics used in the light valve projector.

A simple schlieren system would consist of a sheet of opaque material with a narrow slit cut in it, a lens, and a narrow bar. The dimensions of the slit and bar are such that they can be situated so that the slit is imaged on the bar and vice versa. If the slit is illuminated from the rear it can be seen that the bar and the bar only will be illuminated by the light emitted from the input slit. With a phase grating placed between the lens and the output bar some of the light incident upon the grating will be diffracted so that it passes by either side of the bar. By controlling the amount of light that is diffracted the amount of light that is collected by a projector system to form an image of the grating is controlled as well.

The system used in the projector is somewhat more sophisticated

than the system described above.

The single input slit is replaced by a series of slits. The single output bar must, of course, be replaced by a series of bars. Each output bar is still placed at the image of an input slit so that the light diffracted by the grating passes through the open area between the output bars.

APPENDIX B

AN ELECTRICAL ANALOGY FOR THE PROJECTOR

By combining the analogies with network theory that were observed during the course of the analysis, an electrical analogy has been devised for the projector.

It was seen that the sinusoidal grating produced diffraction orders that were very similar to the sidebands produced by frequency or phase modulation. Consequently the grating is represented by a phase modulator in the analogy. The modulating signal is produced by an amplitude modulator. The carrier frequency of the latter modulator represents the grating frequency. The input represents the video information which is to be displayed.

Displacement along the output bars was transformed into a spatial frequency domain in the analysis. Consequently output bars are replaced with filters in the analogy. The most representative filter would be a comb filter with a pass band centered on each sideband or diffraction order that is to be utilized. This would require a separate filter for each output bar arrangement to be studied. In addition, a comb filter with the proper characteristics (phase shift proportional to frequency and no attenuation in the

pass band) would be quite impracticle and expensive. A more practicle method of investigating the system response would be to replace the comb filter with a spectrum analyzer.

Since the input and output bars are images of one another, the planes in which both are situated represent frequency domains. Consequently, the coherent line source analyzed could be represented by a discrete frequency. This would be used as the carrier for the phase modulator.(The source located on the system axis used in the analysis would represent a d. c. carrier) The source consisting of a series of line sources suggested in the conclusions of the report could be produced by passing white noise through a band pass filter. If the latter scheme were used as an input for the modulator, an analogy for the actual system could be produced by using a comb filter in the input and the complimentary filter (a stopband in one is the pass band of the other) in the output. The signal from the output filter would have to feed into a squaring circuit before a signal representing the image seen by the eye would be produced.

A block diagram of the analogous system showing both inputs is shown in Figure 17.

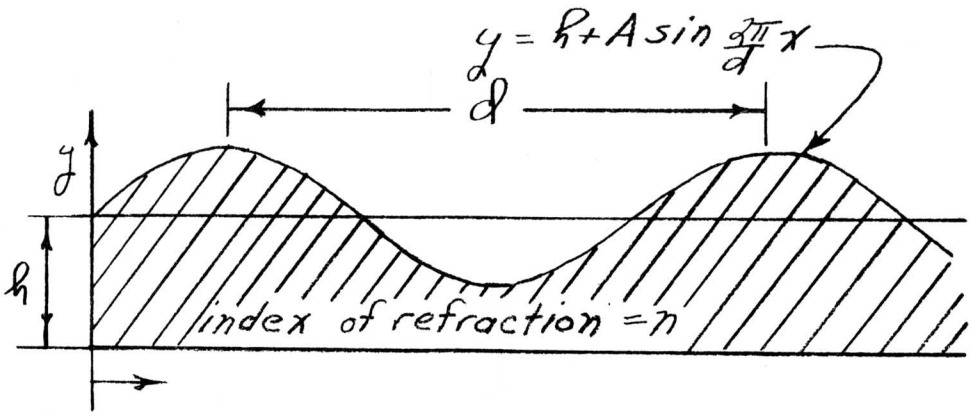

Sinusoidal Grating Cross-Section

Figure 1

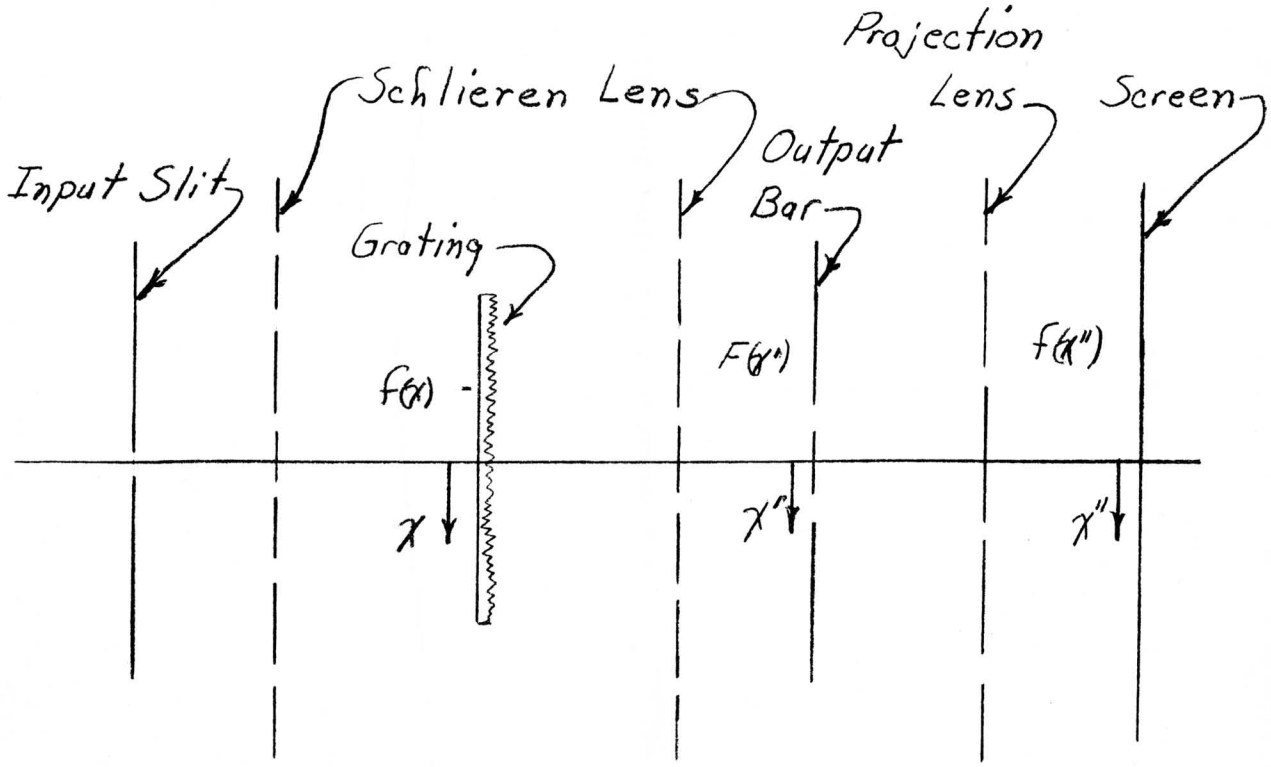

Projector Model

Figure 2

Instantaneous Conversion Efficiency vs. Depth of Modulation for Various Diffraction Orders

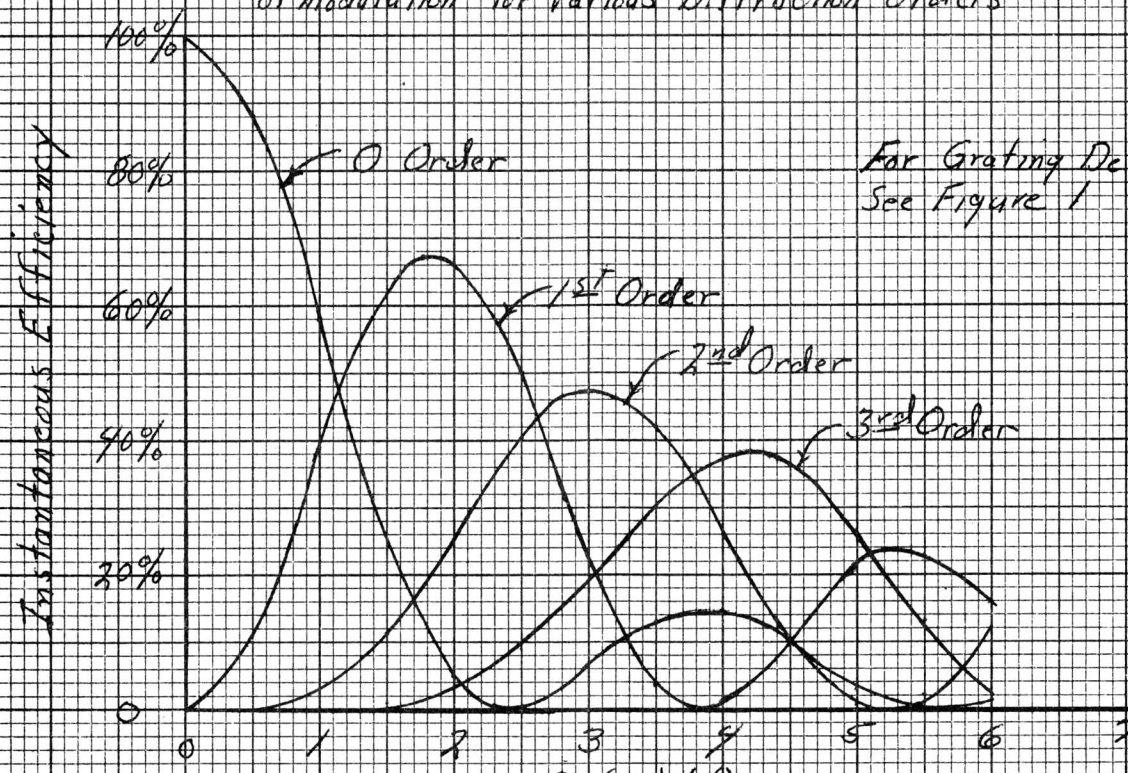

Figure 3

Instantaneous Efficiency for Various Combinations of Orders

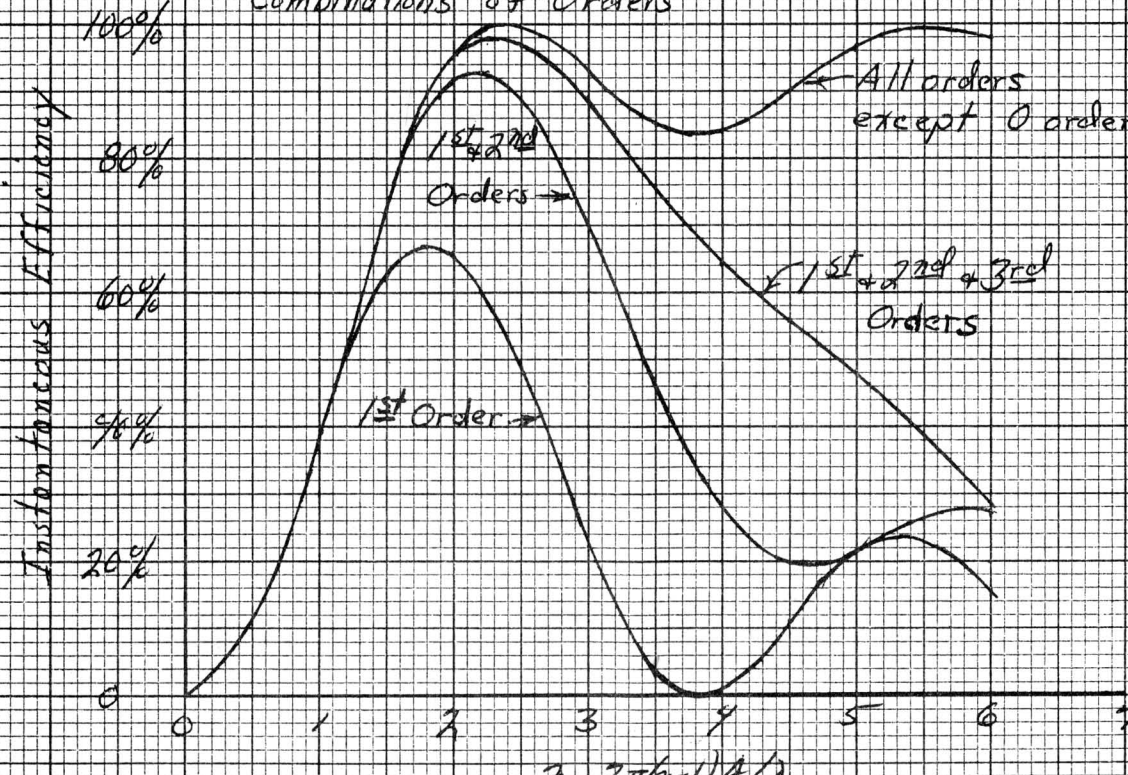

Figure 4

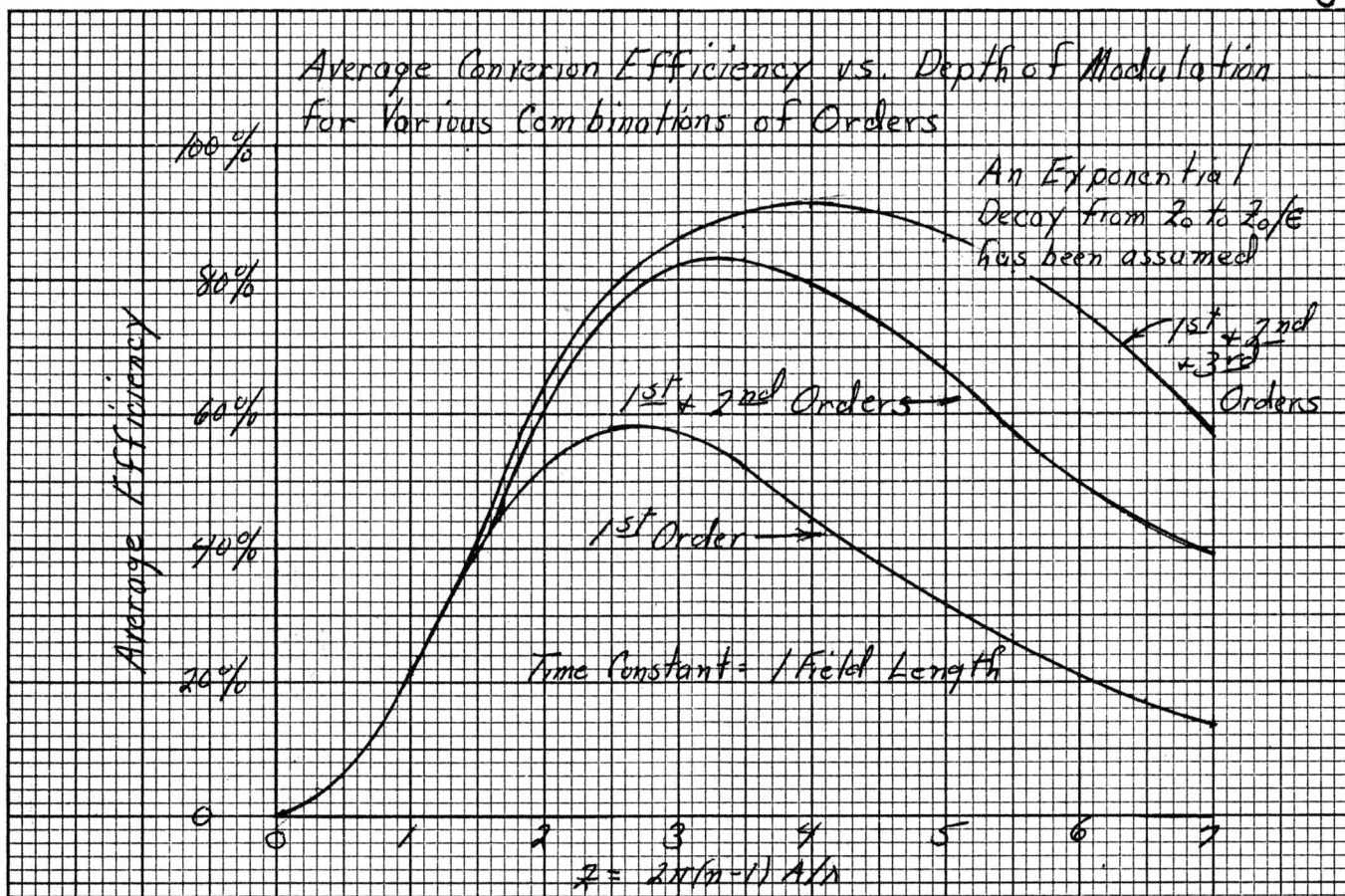

Figure 5

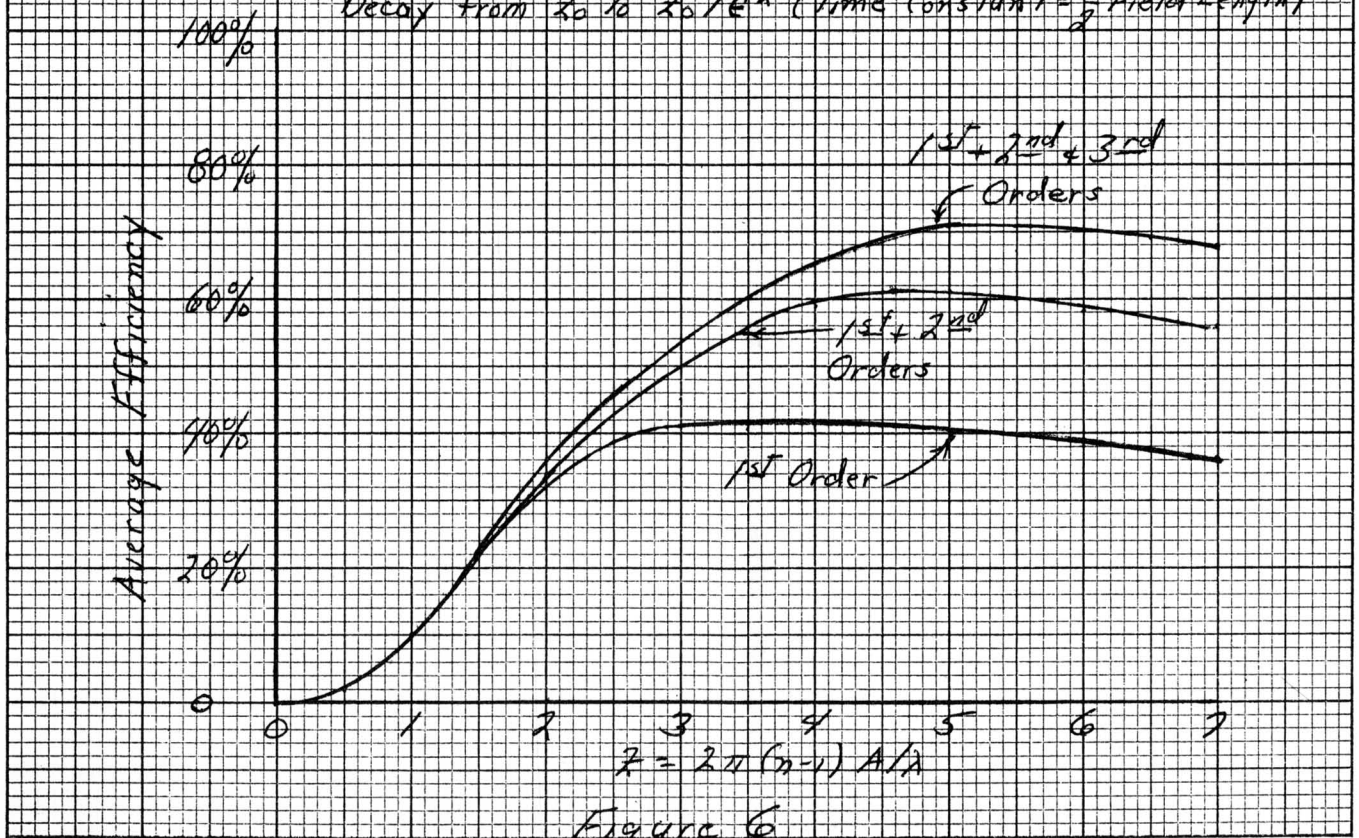

Figure 6

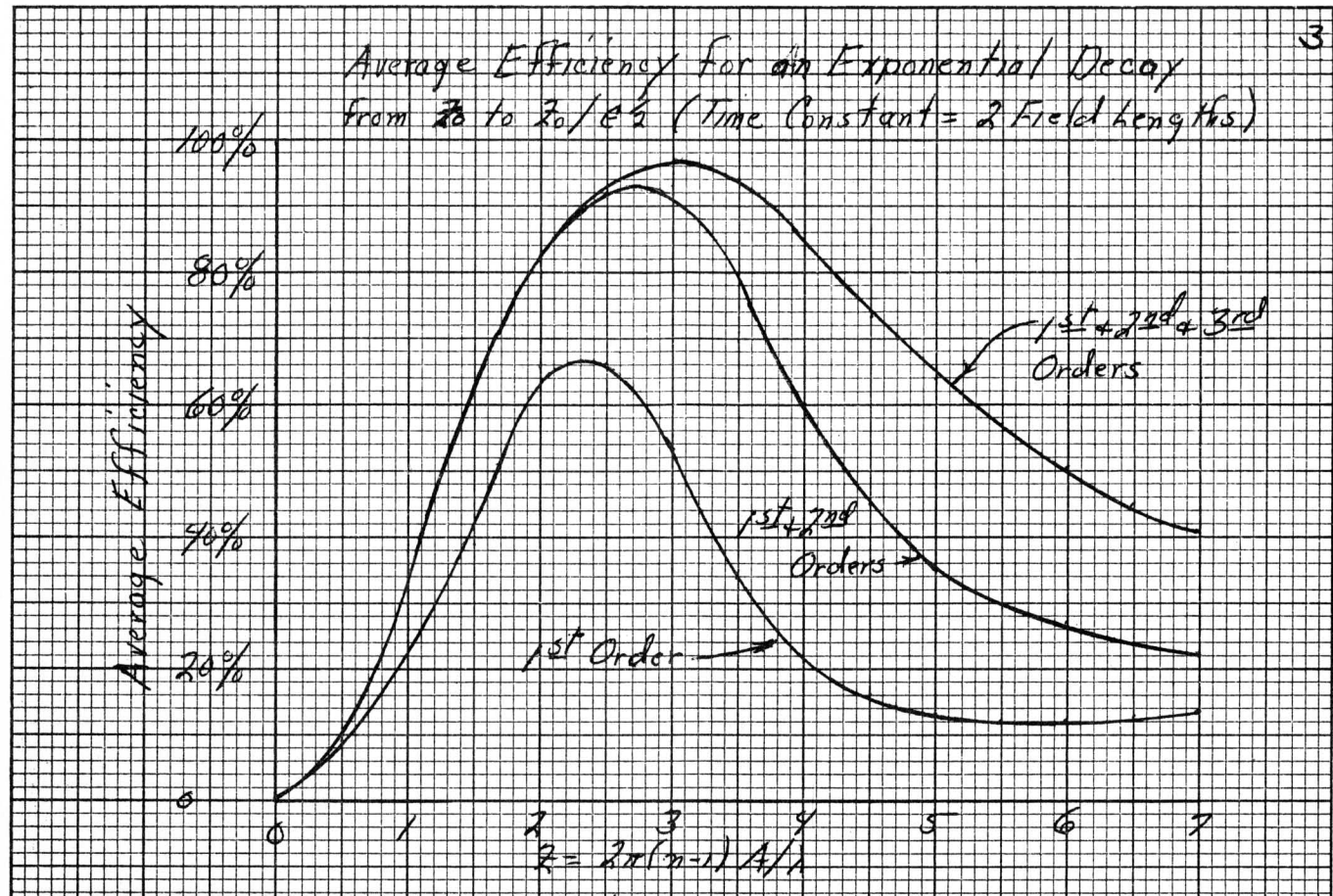

Figure 7

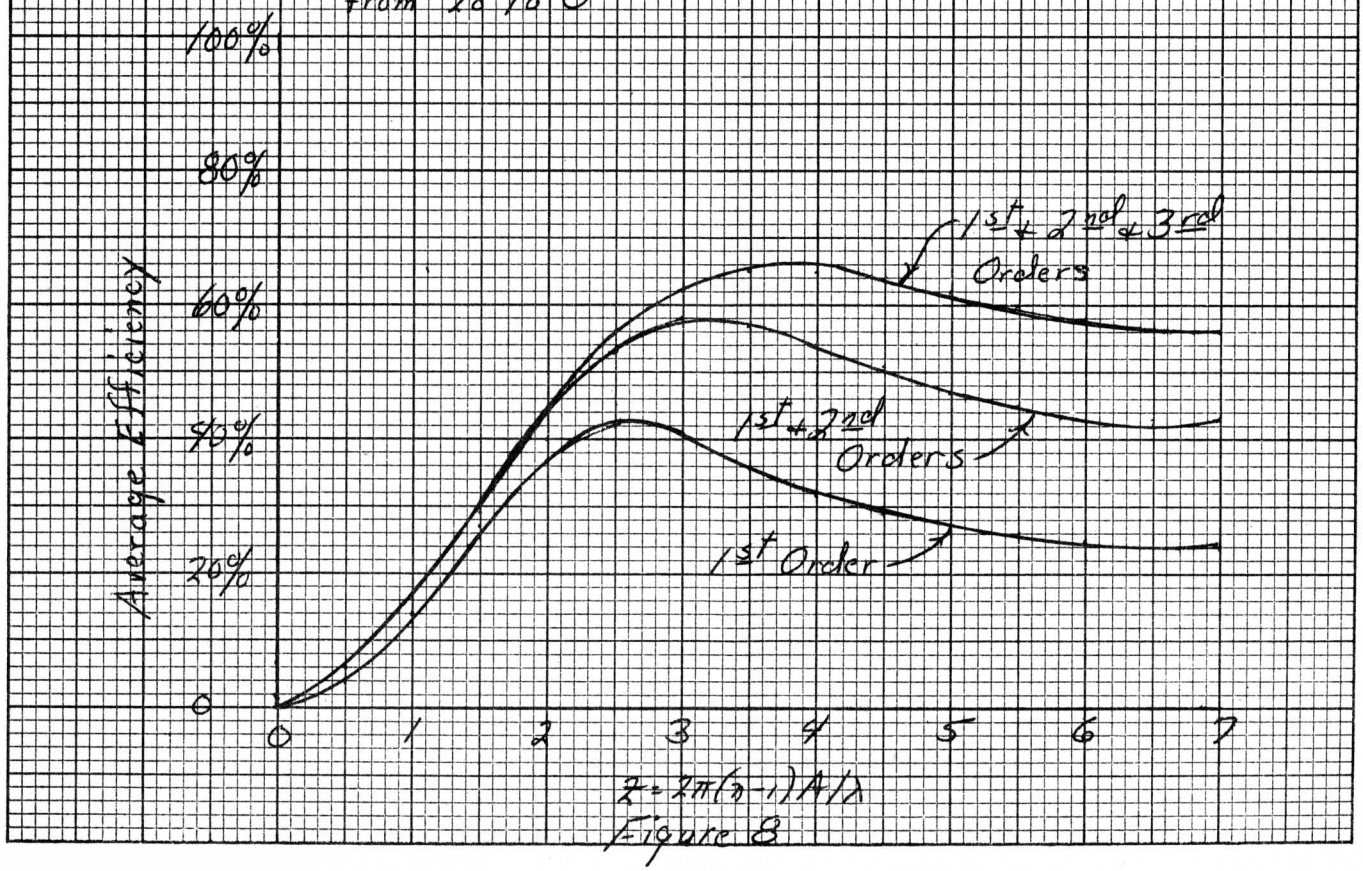

Figure 8

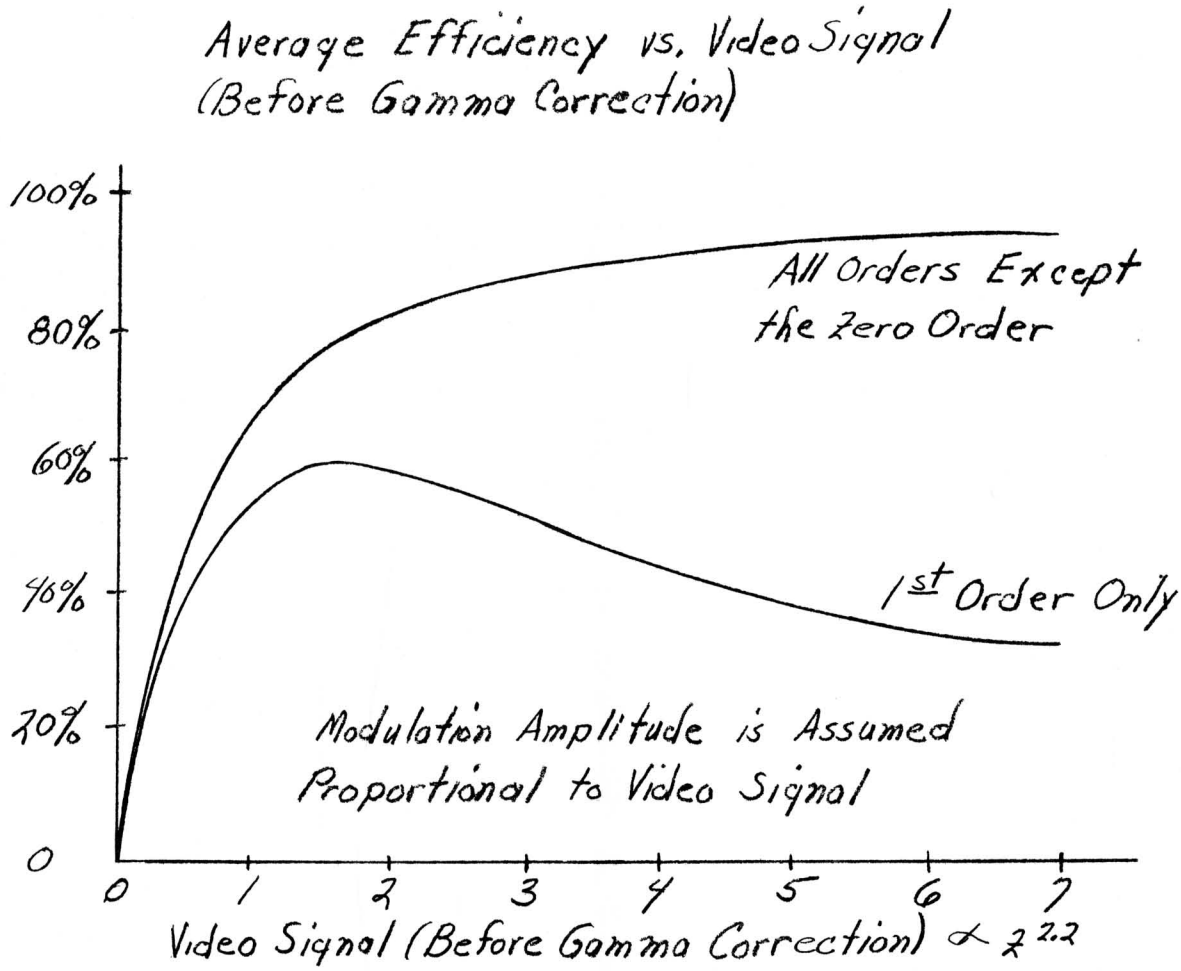
Average Efficiency vs. Video Signal
(Before Gamma Correction)
100%
80%
60%
40%
20%
0
All Orders Except
the Zero Order
1st Order Only
Modulation Amplitude is Assumed
Proportional to Video Signal
0
1
2
3
4
5
6
7
Video Signal (Before Gamma Correction) ∝ z 2.2

Figure 9

Response of Projector to a Step Function
(Video Signal)

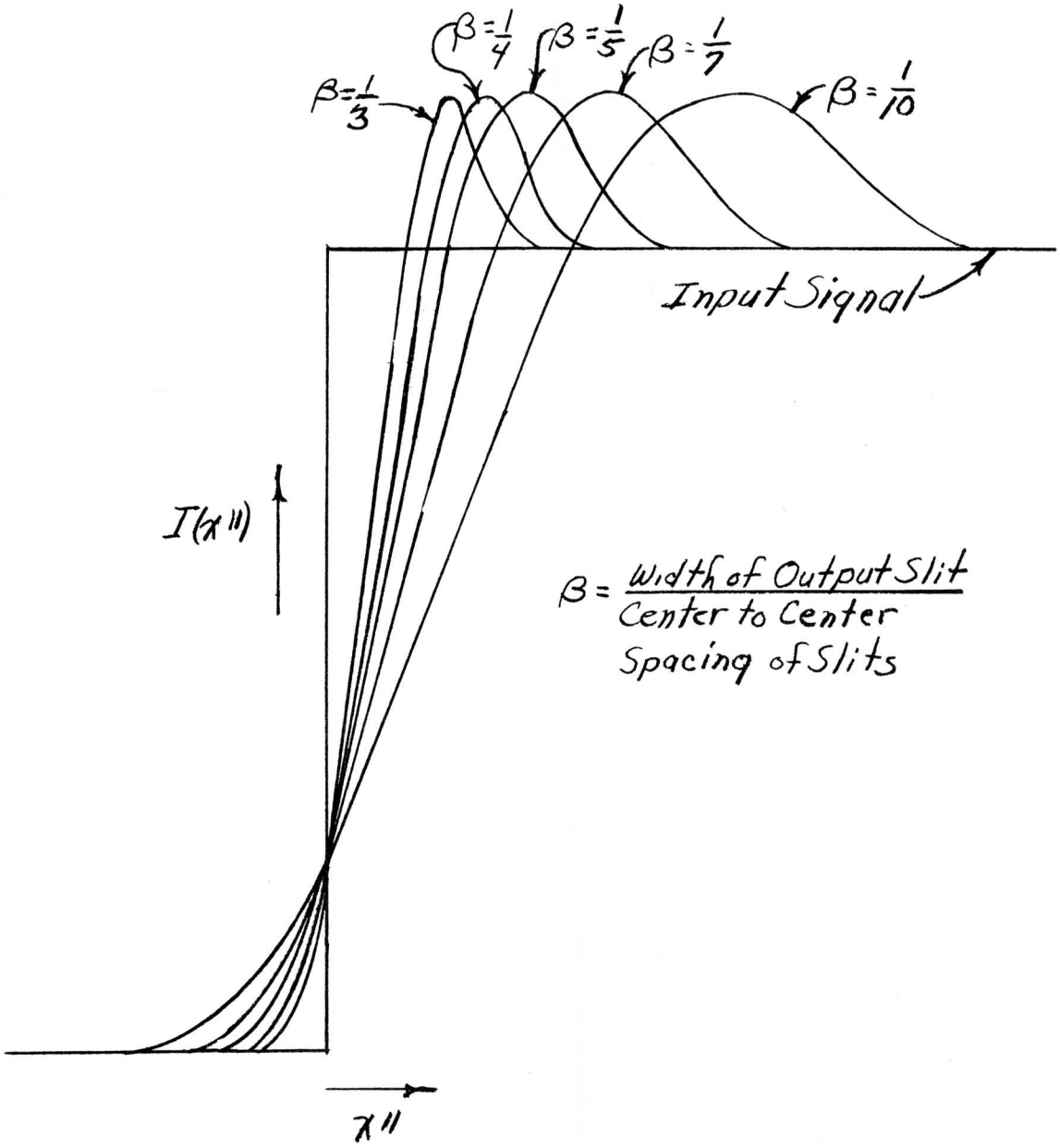

Figure 10

Response of Projector to a Single Pulse
(Video Signal)

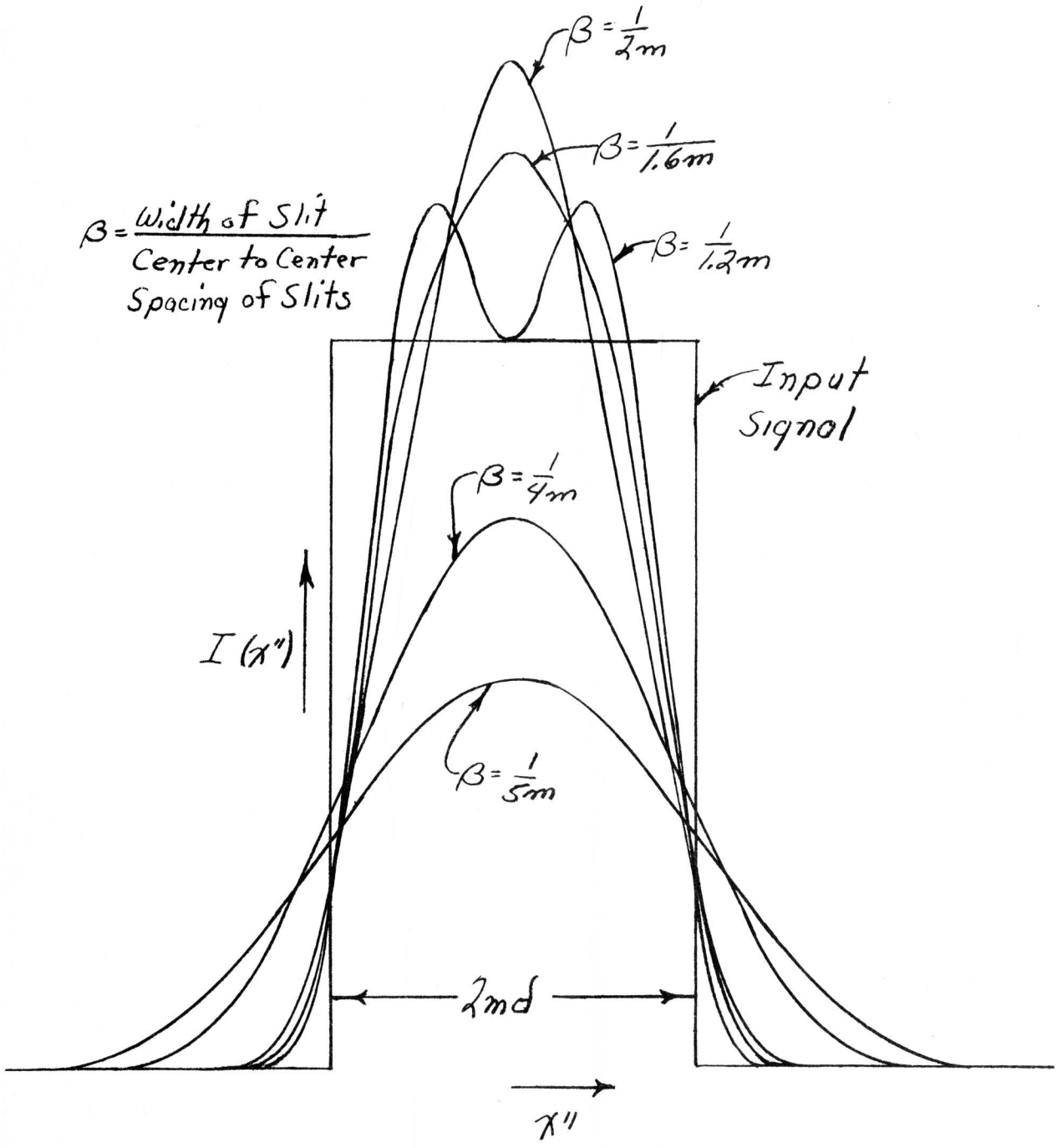

Figure 11

Response of Projector to a Double Pulse
(Video Signal)

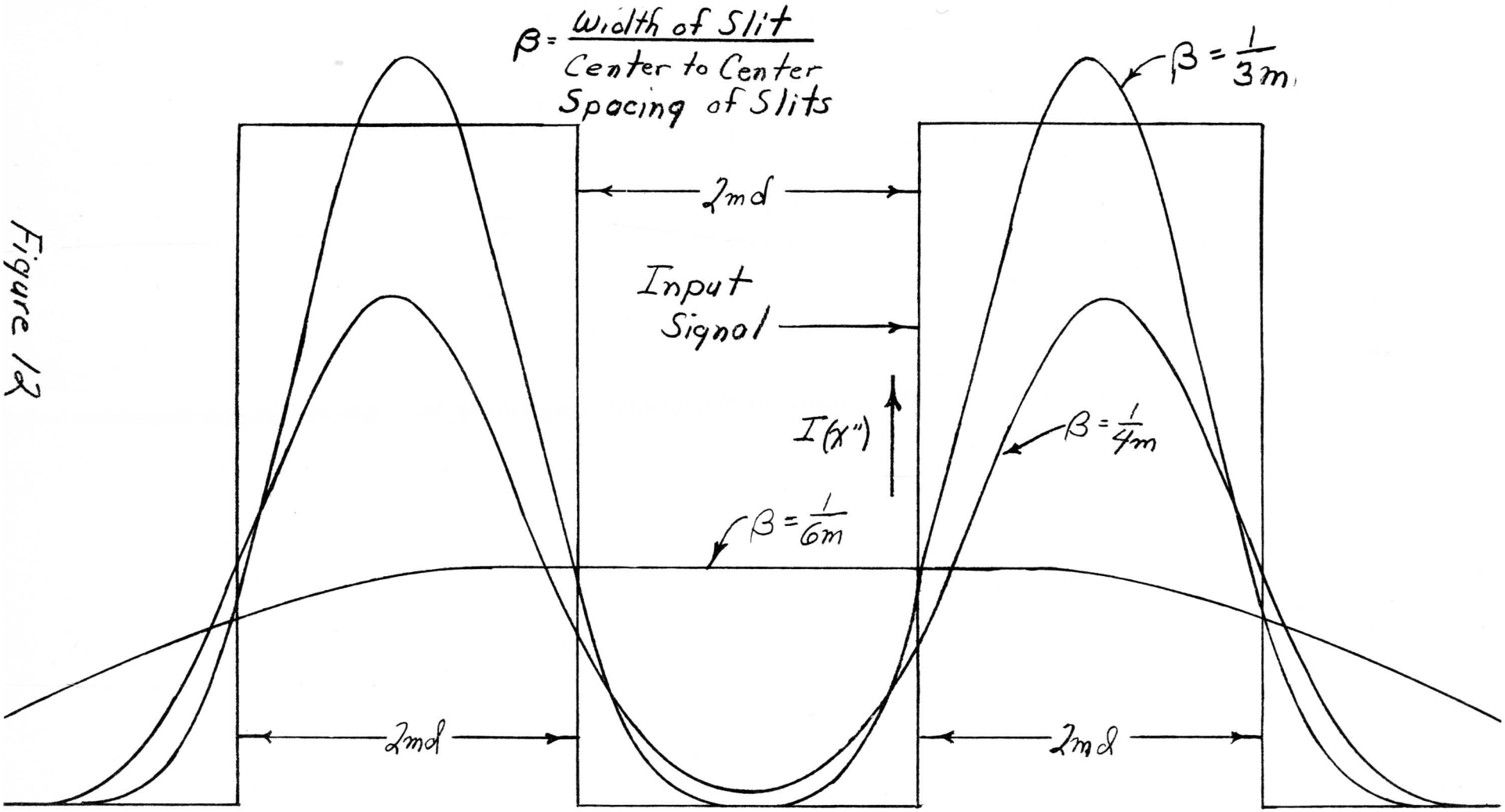

Figure 12

Figure 12

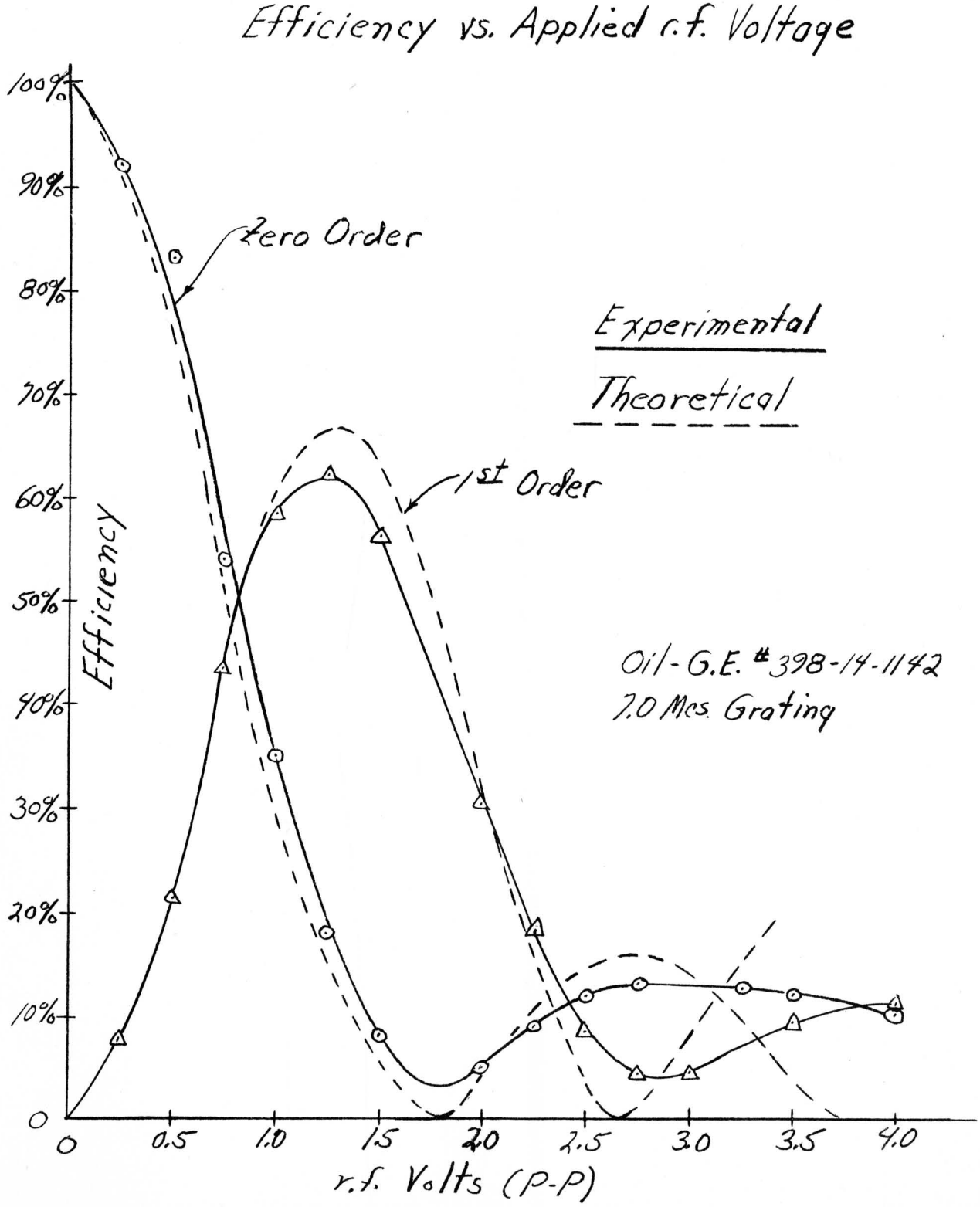
Efficiency vs. Applied r.f. Voltage
100%
90%
80%
70%
60%
50%
40%
30%
20%
10%
0
Efficiency
Zero Order
1st Order
Experimental
Theoretical
Oil - G.E. # 398-14-1142
7.0 Mcs. Grating
0
0.5
1.0
1.5
2.0
2.5
3.0
3.5
4.0
r.f. Volts (P-P)

Figure 13

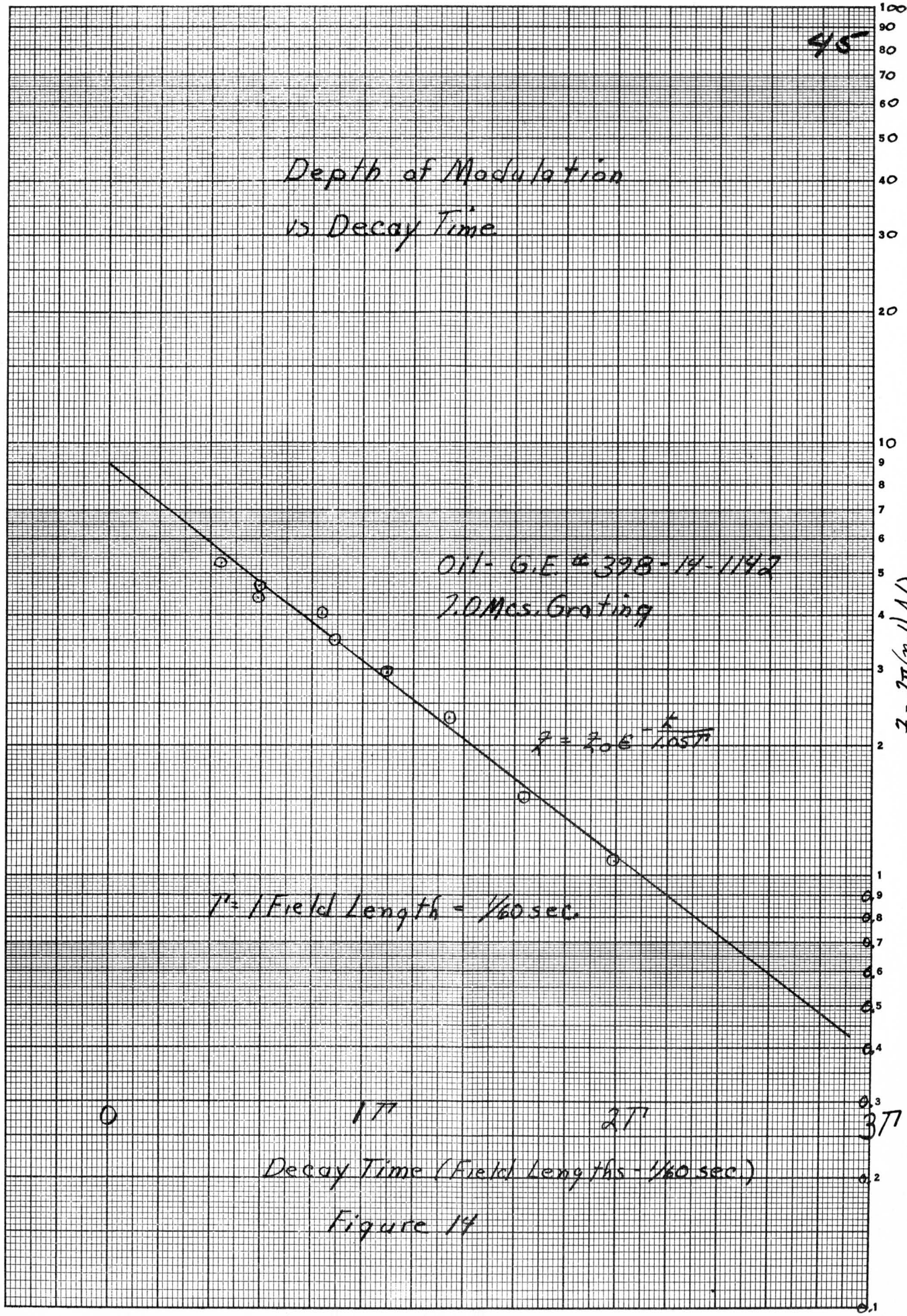

Figure 14

Modulation Depth vs.
Applied r.f Voltage

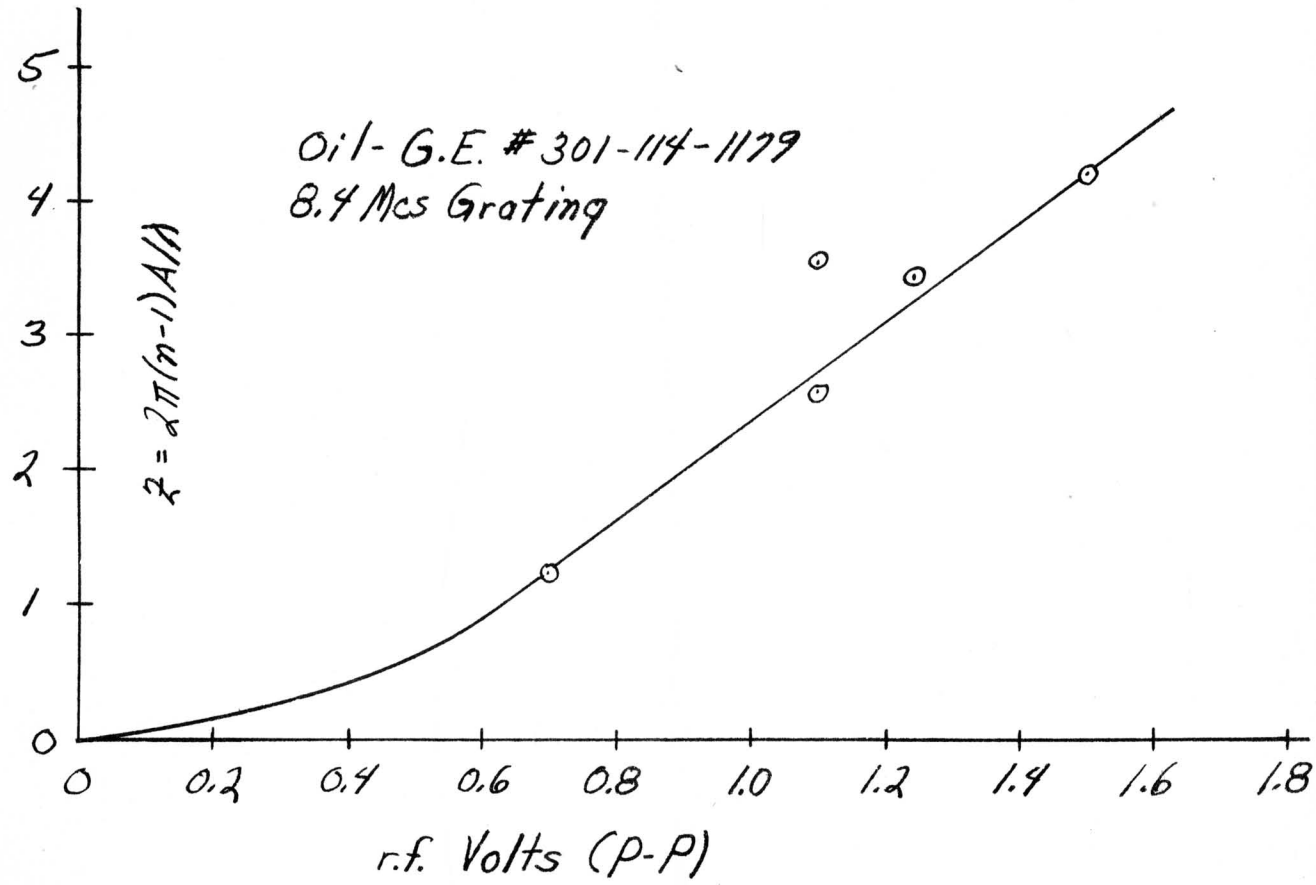

Figure 15

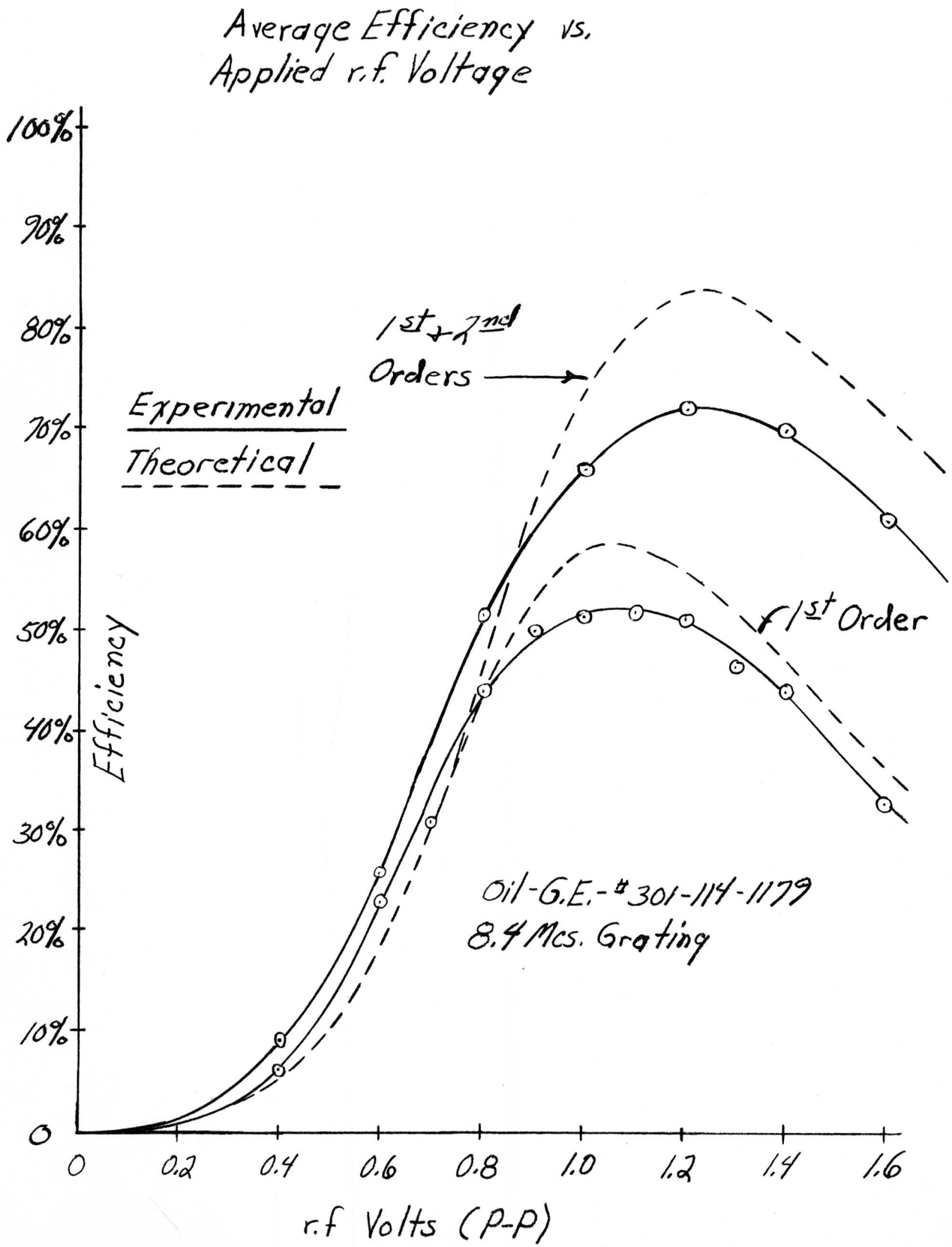
Average Efficiency vs.
Applied r.f. Voltage
100%
90%
80%
70%
60%
50%
40%
30%
20%
10%
0
Efficiency
1st + 2nd Orders
Experimental
Theoretical
1st Order
Oil-G.E.-#301-114-1179
8.4 Mcs. Grating
0
0.2
0.4
0.6
0.8
1.0
1.2
1.4
1.6
r.f Volts (P-P)

Figure 16

Projector Analog

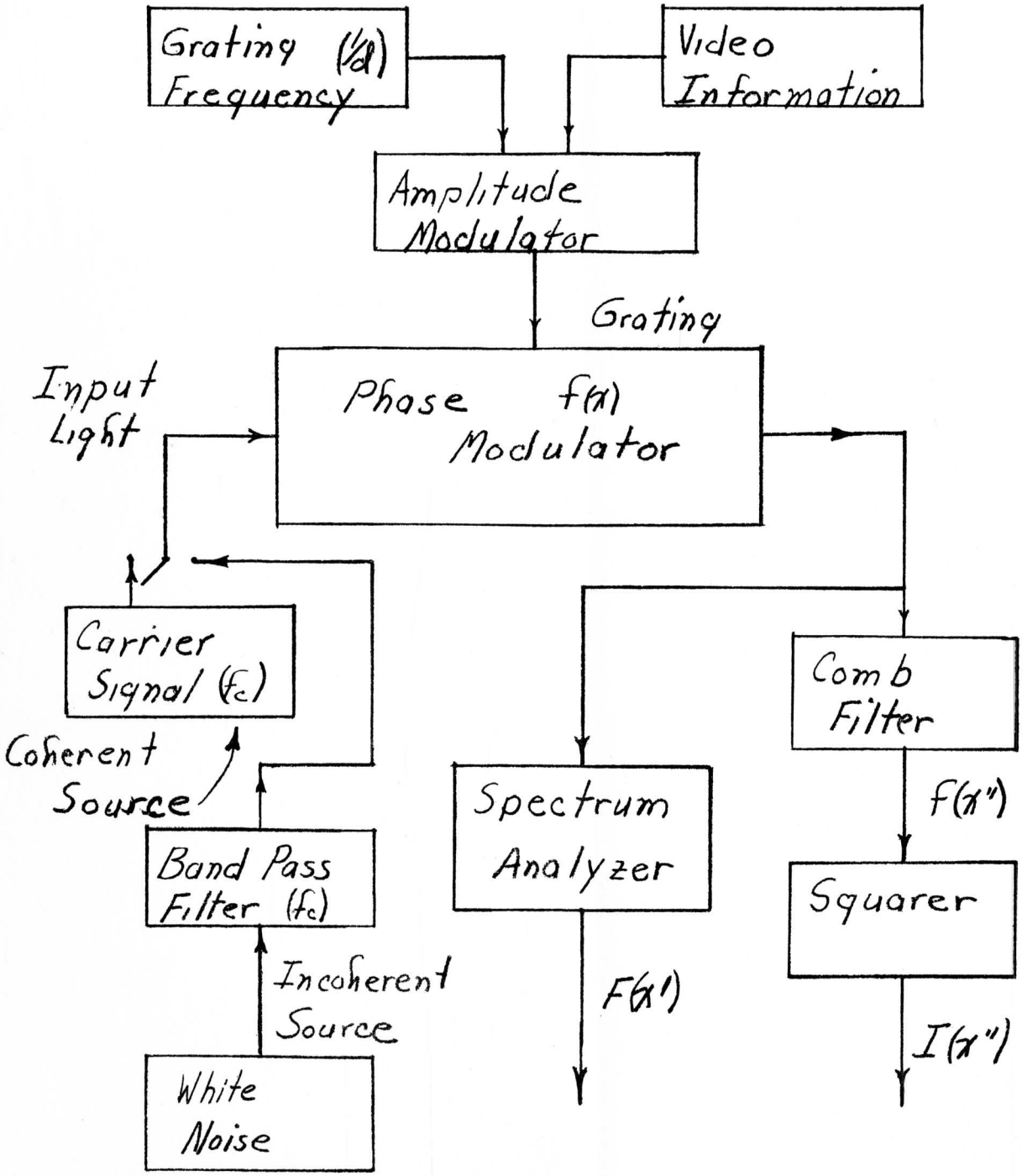

Figure 17

BIBLIOGRAPHY

BOOKS

Born, Max and Wolf, Emil, Principles of Optics. New York, Pergamon Press, 1959.

Goldman, S., Frequency Analysis, Modulation and Noise. New York, McGraw-Hill, 1948.

Goldman, S., Transformation Calculus and Electrical Transients. New York, Prentice-Hall, 1949.

Hildebrand, F. B., Advanced Calculus for Engineers. New York, Prentice-Hall, 1948.

Jahnke and Emde, Tables of Functions. New York, Dover Publications, 1943.

Jenkens and White, Fundamentals of Optics, 3rd Edition. New York, McGraw-Hill, 1957.

REPORTS

DeJager, D., Diffraction Patterns and Sine Wave Response Functions for Slit Type Apertures. General Electric TIS #60GL123, 6/17/60.

Holeman, J. M., Effects of Aperture Slits on the Quality of Projected Image. General Electric TIS #60FL169, 8/22/60.

Horsch, J. R., Lens Utilization in Coherent Optical Data Processing. General Electric TIS #R60 ELS-21, 3/15/60.

O'Neill, E. L., The Analysis and Synthesis of Linear Coherent and Incoherent Optical Systems. Technical Note No. 22. Boston, Optical Research Laboratory, Boston University, 7/55.

O'Neill, E. L., Selected Topics in Optics and Communications Theory. Boston, Physical Research Laboratory ITEK Corporation, 9/58.

Pole, R. V., An Optical Analysis of Surface Deformation Recordings. General Electric TIS #DF59 ELS-82, 9/15/59.